What can be deduced about the structure of *Shaker* from available data?[1]

Benoît Roux,
Weill Medical College of Cornell University,
1300 York Ave, New York 10021

Abstract

Voltage-gated K^+ channels are transmembrane proteins that control and regulate the flow of K^+ ions across cell membranes in response to changes in membrane potential and are essential for the propagation of action potentials in the nervous system. Detailed 3d structures are required in order to address the function of voltage-gated K^+ channels. Available experimental results clearly provide specific constraints on the structure of the channel, even though the direct translation of the available information into 3d structures is not trivial. One of the most studied voltage-gated channel is *Shaker*. The goal of this work is to develop a computational approach to construct and refine 3d models of *Shaker* by incorporating and integrating available experimental data. The approach that we use is based on comparative modelization and global conformational optimization using energy restraints extracted from experimental data.

I. Introduction

The activity of voltage-gated ion channels is the basic molecular mechanisms underlying the electrical excitability of nerves and muscles (Hodgkin and Huxley, 1952). Those channels are specialized transmembrane proteins which control and regulate the flow of ions across cell membranes by opening and closing ("gating") in response to changes in membrane potential (Hille, 1992). The first identified and best studied voltage-gated channel is the *Shaker* K^+ channel from the fruitfly *Drosophilia melanogaster* (Tempel et al., 1987); the corresponding Kv channels in mammalians are called Kv1.1 to Kv1.7 (Jan and Jan, 1997). Normally closed at hyperpolarized resting potentials, *Shaker* K^+ channels undergo a conformational transition from a closed to an open state at depolarization potentials (Cha et al., 1999; Glauner et al., 1999).

Studies have shown that *Shaker* and all the channels in the Kv family are similar structurally and functionally. They are formed by four identical or homologous domains or subunit (MacKinnon, 1991). Analysis of the amino acid sequence suggests that each subunit contains six putative

[1]Published in: *"Ion channels: From atomic resolution physiology to functional genomics"*, **Novartis Foundation Symposium 245**, pp. 84-101, G. Bock Editor, John Wiley & Sons Ltd., Chichester (2002).

transmembrane (TM) segments named S1 to S6 (Tempel et al., 1987; Jan and Jan, 1997). The second (S2) and fourth (S4) segments contain several charged residues, which are affected by changes in membrane potential and form part of the voltage sensor controling the gating of the channel (Papazian et al., 1991; Liman et al., 1991; Logothetis et al., 1992; Aggarwal and MacKinnon, 1996; Seoh et al., 1996; Yellen, 1998; Bezanilla, 2000). The part of the protein forming the pore region responsible for the selectivity and conduction of K^+ ions is located between S5 and S6 of a subunit in a region which contains the essential amino acid "signature sequence" TTVGYGD common to all K-channels (Heginbotham et al., 1992, 1994).

Although a growing body of information is available about *Shaker* as well as other voltage-activated channels in the Kv family, the only ion channel for which a structure at atomic resolution is currently available is the KcsA channel from *Streptomyces lividans* (Doyle et al., 1998). The main features of the crystallographic structure is shown in Figure 1. The channel is made of four identical subunits disposed symmetrically around a common axis corresponding to the pore (only two are shown in the figure). Although the monomer of KcsA are formed by only two transmembrane helices, the amino acid sequence is, in fact, very similar to the segment S5-S6, which is conserved in eukaryotic voltage-gated channels such as *Shaker* (Doyle et al., 1998; Schrempf et al., 1995; Cortes and Perozo, 1997). Furthermore, a combination of structural and functional data with neurotoxin from scorpion indicate the extracellular vestibule of KcsA is structurally very similar to *Shaker* (MacKinnon et al., 1998).

In the absence of a detailed atomic structure, extensive studies using a variety of experimental approaches including, electrophysiology, site-directed mutagenesis, resonance energy transfer, and electron microscopy, have been used to probe the structure and function of the *Shaker* K^+ channel. Undoubtedly, many of the experimental results obtained so far put very specific constraints on the structure of *Shaker*, though often indirectly. Nonetheless, the direct translation of all the available information into a three-dimensional (3D) structure is not straightforward. The purpose of the present work is to develop a computational approach to construct and refine 3D models of *Shaker* by incorporating and integrating all available experimental data. The approach that we use is based on comparative modelization and global conformational optimization using energy restraints extracted from experimental data. Given the limited amount of information presently available, we do not expect to converge towards a unique "best" model of *Shaker*. Instead, we seek to delineate and clarify, as objectively as possible, the current state of the knowledge about

Shaker by generating an ensemble of plausible models which are consistent with the available data. Our hope is that such an ensemble of 3D models can play a useful role in the design of future experiments by indicating the areas of greatest uncertainty in the structure, by helping to examine the spatial relationship between functionally important residues, and by revealing inconsistencies between different experiments results.

II. Assumptions

The general topology of a subunit of *Shaker* is illustrated schematically in Figure 2. In particular, it is assumed that the segment S1 to S4 are in an α-helical conformation and that the central pore formed by S5-P-S6 is structurally very similar to the crystallographic structure of the KcsA K^+ channel. Although those assumptions are reasonable and supported by experimental evidence at the present time, some of them might turn out to be incorrect in the future. Nonetheless, such simplifications are necessary at this point.

a) Helical conformation of the TM segments S1 to S4

It is assumed that the transmembrane segments S1 to S4,

S1 (226-247): ARVVAIISVFVILLSIVIFCLE
S2 (279-300): FFLIETLCIIWFTFELTVRFLA
S3 (311-332): VMNVIDIIAIIPYFITLATVVA
S4 (358-380): LAILRVIRLVRVFRIFKLSRHSK

are in an α-helical conformation and are roughly perpendicular to the membrane plane, though some tilting of the helix axis is possible.

This hypothesis is supported by a number of observations. Experimental studies have established that isolated fragment corresponding to S4 adopts predominantly an α-helical conformation in methanol and in lipid membranes (Mulvey et al., 1989; Haris et al., 1994; Halsall and Dempsey, 1999). The structure is a random coil in aqueous solution (Haris et al., 1994). Similar studies with TM segment of the sodium (Na) channel have shown that they adopt α-helical structures in detergent micelles (Doak et al., 1996). There are also strong indications that the S1 to S4 segments are α-helical in the channel structure. Ala- (Li-Smerin et al., 2000a) and Trp-scanning

(Monks et al., 1999; Hong and Miller, 2000) mutagenesis studies suggest that S1 and S2 are amphipathic membrane spanning α-helices that interface directly with the lipid membrane. Helical periodicity of functional alteration in the voltage-activation curves and gating kinetics were observed throughout S1 and S2. Trp-tolerant positions in the *Shaker* K^+ channel are clustered on approximately half the α-helix surface, as if the side chains are exposed to the hydrocarbon region of the lipid bilayer (Monks et al., 1999; Hong and Miller, 2000). Similarly, Ala-scanning mutagenesis in the drk1 K^+ channel of S1 and S2 suggest that these segments are relatively simple amphipathic-helices that span the full width of the membrane and make extensive contacts with the lipid membrane (Li-Smerin et al., 2000a). The observations are more complex for the S3 and S4 segments. In the case of S3, the distribution of Trp-tolerant position is roughly consistent with a helical secondary structure although the results are not as clear towards the extracellular side (Hong and Miller, 2000). Results from Ala (Li-Smerin et al., 2000a) and Lys-scanning (Li-Smerin and Swartz, 2001) with the drk1 K^+ channel suggest that the S3 segment is entirely helical, but that the NH(2)-terminal part interfaces with both lipid and protein, whereas the COOH-terminal part interfaces with water. It has been speculated that a conserved proline at position 322 might induce a kink in the helical segment. Ala-scanning of S4 reveals helical periodicity in only the COOH-terminal region (Li-Smerin et al., 2000a). However, it seems likely that the absence of helical character in the NH2-terminal portion, which is exposed to the intracellular side, results from complexities in the aqueous and protein environment surrounding the segment.

b) Structure of the central pore S5-P-S6

It is assumed that the conformation of the central pore of *Shaker*, formed by the S5-P-S6 segment, is very similar to the crystallographic structure of KcsA (Doyle et al., 1998). This is a very reasonable assumption given the high sequence similarity of the core of *Shaker* and the KcsA bacterial channel:

```
KcsA:      ALHWRAAGAATVLLVIVLLAGSYLAVLAERGAPGAQLITYPRALWWSVETATTVGYGDLYPVTLWGRCVAVVVM
Shaker:    -ASMRELGLLIFFLFIGVVLFSSAVYFAEAGSENSFFKSIPDAFWWAVVTMTTVGYGDMTPVGFWGKIVGSLCV
               *  *     * * ..  *     ** *. ..  . * * **.* * *******.   **  **. *  ..

KcsA:      VAGITSFGLVTAALATWFVGREQ
Shaker:    VAGVLTIALPVPVIVSNFN----
           ***. .  *    . . *
```

for 93 residues, the sequence identity is 31 and the sequence similarity is 15 for a global sequence homology of 49%. This high similarity makes *Shaker* an excellent candidate for a successful comparative modeling using the KcsA structure as a template (Fiser et al., 2000). The structural similarity of *Shaker* relative to KcsA is also supported by experiments: AgTx2 binds to the KcsA channel, demonstrating that this prokaryotic K-channel has the same pore structure as that of *Shaker* (MacKinnon et al., 1998), and the chemical modifications of cysteines located along S6 by soluble thiol agents are generally consistent with the accessibility of the corresponding residues in KcsA (Liu et al., 1997). Because the KcsA K^+ channel is in a closed conformation (Roux et al., 2000), the crystallographic structure is probably a better model for the closed state of *Shaker*. Nonetheless, although it appears to be very reasonable, the assumption that the S5-P-S6 core of *Shaker* is structurally similar to KcsA can be wrong for some regions of the structure. In particular, the sequence similarity is much smaller near the end of S6, which may indicate that the structure of this region differ from KcsA. In particular, S6 contains the motif Pro-Val-Pro at position 473-474-475, which is known to perturbe α- helices considerably (Barlow and Thornton, 1988; von Heijne G, 1991). In addition, recent results from blocker protection in the pore of a voltage-gated K^+ channel suggests that the structure of Kv channels differs from that of the KcsA by the introduction of a sharp bend in the S6 helices (del Camino et al., 2000).

III. Experimental Data

a) Intragenic suppression

Using an intragenic suppression strategy, Tiwari-Woodruff et al. (1997) showed that charge reversal mutations of E283 in S2 and K374 in S4 disrupt maturation of the protein. Maturation was specifically and efficiently rescued by second-site charge reversal mutations, indicating that electrostatic interactions exist between E283 in S2 and R368 and R371 in S4, and between K374 in S4, E293 in S2, and D316 in S3. Further investigation of those mutants showed that the interaction between K374 in S4 and E293 in S3 and D316 in S3 is important for the closed state whereas the interaction between E283 in S2 and R368 and R371 in S4 is probably important for the open state (Tiwari-Woodruff et al., 2000).

b) Resonance energy transfer

Using lanthanide-based resonance energy transfer (LRET) to measure distances between *Shaker* potassium channel subunits at specific residues, Cha et al. (1999) determined the distance between site-speficic labeled monomer. Specific sites in the channel were fluorescently labelled by substituting a cysteine for particular residues and attaching a cysteine-reactive compound of either a donor (a terbium-chelate maleimide, TbM) or an acceptor (fluorescein maleimide, FM). The intersubunit distances were evaluated using the relaxation time constant of acceptor-sensitized emission and donor emission without an acceptor. The distances estimated with this method are accurately determined because the lanthanide donor is in fast orientational averaging. For example, the distance measured across the pore at F425 is in excellent accord with the the distance between the carbon α for the corresponding residue in the Xray structure of KcsA. Furthermore, it was shown that the distances deduced independently from the energy transfer between the nearest and opposite subunits in the tetramer were consistent with Pythagoras's theorem. The most important distances measured between two monomers on opposite side of the tetramer were 46 Å for D273, which is located near the extracellular end of S2, 41 Å for N353 near the extracellular end of S4, and 45 Å for V363 in the middle of S4.

c) Tethered pore blockers

Blaustein et al. (2000) have used a clever method based on a series of compounds of varying length ending with a quaternary ammonium (QA) pore blocker. To located the S1-S4 segments relative to the central pore these compounds were tethered to specific test residues using site-directed cyteine mutations. By examining the probability of blockade as a function of the length of the compounds, it was shown that the extracellular ends of S1 and S3 are approximately 30 Å from the the external opening of the pore while the the S3-S4 linker is, at 17-18 Å from the pore.

d) Scanning mutagenesis

Miller and co-workers have performed site-directed substitution of all residue in S1, S2 and S3 probing for significant functional changes (Monks et al., 1999; Hong and Miller, 2000). The function of the channel was significant affected after substitution of Trp at the following positions: A226, R227, V229, A230, S233, V234, I237, L238, S240, I241, I243, F244, and C245 for S1, E283, C286, I287, F290, E293, L294, R297, A300 for S2, M312, N313, I315, D316, A319, I320, P322, Y323, F324, L327, V330, V331 for S3. The function of the channel was not significantly affected by similar subtitutions at other positions. Helical periodicity of functional alteration in the voltage-activation curves and gating kinetics were observed throughout S1 and S2. A similar result was obtained with S3, although the distribution of Trp-tolerant position is not as clear towards the extracellular side. The Trp-tolerant positions are clustered approximately on one face of the putative α-helical segments, as if those side chains were exposed to the hydrocarbon region of the lipid bilayer. The results are consistent with Ala-scanning mutagenesis studies on a related Kv channel (Li-Smerin et al., 2000a; Li-Smerin and Swartz, 2001). Interestingly, comparison of the amino acid sequence of several channels in the Kv family showed that the Trp-tolerant sites exhibit a high level of sequence variability, whereas the Trp-intolerant sites are highly conserved. This observation further reinforces the suggestion that Trp-tolerant residues are exposed to the lipids hydrocarbon, while the Trp-intolerant residues are involved in protein-protein contacts.

Recently Sokolova et al. (2001) obtained the 3D structure of the complete *Shaker* channel at 25 Å resolution using single-particle electron microscopy. The 3D map clearly shows that the *Shaker* channel has a two-domain architecture with a transmembrane domain, corresponding to S1-S6, and a soluble domain corresponding to the T1 domain attached to the transmembrane domain by thin connectors. This two-domain architecture is consistent with the "hanging gondola" model proposed by Kobertz et al. (2000). Although the image is still at very low resolution, it shows that the transmembrane section of the channel has the shape of a compact square of roughly 70 Å on the side.

IV. Modelization Procedure

a) The TM segments S1-S4

The S1-S4 segments were constructed as ideal α-helices and then further refined by energy minimization. A rather conservative definition of helical segments S1 to S3, with only 21-22 residues, was used in the modelization to avoid "over" constraining the system with long α-helical TM segments. In the case of S4, the helical segment was constructed as an α-helix from residue 350 to 380 based on the mutagenesis results of Gonzalez et al. (2000).

Planar energy restraints were applied to keep the ends of the TM segments outside a 30 Å thick hydrophobic slab and maintain the orientation of the helical segments. It is implemented as a half-harmonic potential with a force constant of 10 kcal/mol/Å^2. This energy restraint keeps the helices roughly perpendicular to the membrane while allowing some tilting of the helices, in agreement with the orientation of TM helices in membrane proteins of known structure (Bowie, 1997).

For the sake of simplicity, the S1-S2 (31 residues), S2-S3 (10 residues), S3-S4 (17 residues), and S4-S5 (10 residues) linkers between the TM segments were not included explicitly. Instead, a simple half-quadratic restraint of 10 kcal/mol·Å^2 was used to limit the maximum distance between the C- and N-termini of the ends of adjacent TM segments (S1-S2, S2-S3, S3-S4, and S4-S5). A maximum distance of 25 Å was used for S1-S2 linker while a distance of 10 Å used to the other loops. Experimental studies have shown that the S3-S4 linker can be shortened from 17 to the 5 amino acids closest to S4 without disrupting the function and the gating of the channel (Sorensen et al., 2000), indicating that the C- and N-termini of the helices are probably close in space.

b) The central pore

The three-dimensional model of the central pore of *Shaker* was constructed on the basis of its sequence similarity with KcsA for which there is a crystallographic structure. The program **MODELLLER v4** (Sali and Blundell, 1993) was used to produce 3D homology-based models by satisfaction of spatial restraints. Its ability to produce high quality 3D atomic structures based on sequence similarity has been evaluated (Sali et al., 1995). The segment S6 was modeled as a straight helix, even though there are indications of a sharp bend (del Camino et al., 2000). The

ideal four-fold symmetry of the tetrameric channel models was imposed with energy restraints. Fifty 3D models were generated. The best model was kept and then further refined with energy minimization of the side chains.

c) Distance energy restraints

Several pieces of information can be translated as constraints on the range of allowed distances between different parts of the structure. This information is incorporated into the modelization as artificial distance-energy restraints which takes the form of a quadratic function. All the restraints that were used are given in Table 1. Energy restraints corresponding to the salt bridge between E293 in S2, D316 in S3 and K374 in S4 were applied (Tiwari-Woodruff et al., 1997, 2000). A maximum distance of 3 Å between the side chain atoms having the ability to form the salf bridge was applied with a harmonic force constant of 20 kcal/mol·Å^2. Restraints corresponding to the salt bridge between E283 in S2 and R368 and R371 in S4 were also included. Because those salt bridges are thought to be formed only in the open state (Tiwari-Woodruff et al., 2000), weaker restraints with a force constant of 5 kcal/mol/Å^2 and allowing for a maximum distance of 6 Å were used. The LRET restraints are all applied between subunit A and D, and between subunit B and C. Because the linker residues between the TM segments are not included for the sake of simplicity, the LRET restraint measured for D273 which is part of the S1-S2 linker was transfered to F279 at the end of S2.

d) Lipid-exposed residues

A directional energy restraint was applied to force the orientation of S1-S3 such that the Trp-tolerant residue point away from the core of the structure towards the lipid hydrocarbon region. The energy restraint takes the form of a pseudo dihedral angle,

$$E_{\text{expo}}(\phi) = K_{\text{expo}} \cos(\phi - 180) \tag{1}$$

where ϕ is the angle between the center of mass of the lipid-exposed residues and the protein-exposed residues projected onto the XY plane. The restraint was applied to all side chain atoms of the buried and exposed residues to insure proper orientation with respect to the core structure S5-S6. The force constant of the pseudo-dihedral energy restraint K_{expo} was 10 kcal/mol/rad^2.

An energy restraint based on a rigorous calculation of the solvent-accessible-surface-area (SASA) could be used in the later stage of the structural refinement. However, the calculation of the exact SASA (Richards, 1977) is computationally much more expensive than the approximation used here, and is unnecessary at this stage.

e) Conformational sampling and simulated annealing procedure

Initially, S1 to S4 are disposed around the central pore in arbitrary position and orientation to insure a thorough exploration of all conformational possibilities. To obtain a starting position, each TM segment is rotated around its axis using an an angle picked randomly. The orientation of S1 to S3 is chosen within a 10 degrees window centered approximately such as exposing the Trp-tolerant residues away from the core of the structure whereas the orientation of S4 is completely randomized over 360 degrees. The initial position of S1 to S4 is then chosen randomly within a distance of 20 to 55 Å away from the axis of the pore (with S4 between 20 and 25 Å, S3 between 30 and 35 Å, S2 between 40 and 45 Å, and S1 between 50 and 55 Å) as well as distributed within a 180 degree quadrant centered on their respective monomer.

The random initial models were refined with cycles of molecular dynamics (MD) simulations at 600 K during 100 ps. To maintain constant temperature, the systems were simulated with Langevin dynamics with a friction constant corresponding to a velocity relation time of 1 ps^{-1}. Electrostatic interactions were not included and van der Waals interactions were truncated at 5 Å to reduce the computational cost. To maintain the helical conformation of the S1 to S4 segments an energy restraint based on the root-mean-square deviation was applied on all the backbone atoms (RMSD restraint). The backbone of the central core S5-P-S6 was fixed in space, but the side chains were allowed to move dynamically. The four-fold symmetry of the tetrameric channel was maintained during the simulated annealing procedure using energy restraints. To reduce the steric clashes and accelerate the convergence, the atoms were allowed to move along an unphysical 4th dimension w, i.e., the interatomic distances were calculated as $r = \sqrt{x^2 + y^2 + z^2 + w^2}$ (van Schaik et al., 1993). A harmonic restraint potential with the form $\frac{1}{2}K_{4D}w^2$ was used to progressively project the coordinates back onto the physical three-dimensional space. Lastly, the configuration was refined in 3D for 10 ps at a reduced temperature of 300 K followed by 200 steps of energy minimization.

Generating and refining one *Shaker* model took approximately 2 hours on a Pentium III 850 MHz.

IV. Results and Discussion

A general pattern rapidly emerged from preliminary conformational searches. In particular, it was observed that the S4 segment was localized near the groove between adjacent subunits to satisfy the distance of 45 Å between V363 across the tetramer obtained by LRET (Cha et al., 1999). The LRET restraints distance on F279 and N353 also contributed to this trend. In addition, it was observed that S2 and S3 were generally adjacent to one another, covering S4, and that the position of S1 relative to the rest of the structure was largely undetermined due to the long S1-S2 linker and the lack of distance constraints. The models have extended structures with S1 often being quite distant from the rest which are most certainly incorrect. According to a low resolution electron microscopy map (Sokolova et al., 2001), *Shaker* should have the shape of a compact squared structure of roughly 70 Å on the side. To form a compact structure, S1 should be in proximity to the other segments S2 to S4. Furthermore, all the charged residues of S4 can not be shielded from the lipid environment by only S2 and S3. Because it is unlikely that charged residues would be exposed directly to the hydrocarbon of the membrane, S1 must also be involved in shielding the charges of S4. Lastly, although the inter-helical linkers are sufficiently long to allow a "scrambling" of the TM segments from adjacent subunits, surveys of membrane proteins show that TM helices generally pack against neighbors in the sequence (Bowie, 1997). In order to generate a family of plausible models, we introduced one articificial restraint imposing that the center of S1 be no more than 10 Å away from the center of S4.

Based on these preliminary results, one hundred models were generated according to three plausible topologies shown in Figure 3. The initial position of S4 was chosen within a $\pm$ 10 degrees window centered along the groove between adjacent subunits of the central core to accelerate the conformational search. The position of S1 to S3 is designed to cover S4 from the lipid hydrocarbon: S1-S2-S3, S2-S3-S1, S3-S2-S1, and S1-S3-S2. The 100 models were refined with simulated annealing procedure. One typical model of each type is shown in shown in Figure 4. The 100 model are all equally plausible on the ground of available information. Clearly, the spatial arrangment of S1 to S3 can not be determined without further information from experiments. In the case of the S4 segment, the situation is slightly better and some general trend is emerging. In Figure 5 we show a superposition of the S4 segments from all 100 models with the central pore. The overall root-mean-square deviation on the backbone of all S4 is around 4 to 5 Å. Although

the the orientation of the helix along its main axis is undefined at such resolution, the overal position of S4 is more or less determined by the modelization.

In order to propose useful directions in mutagenesis studies of *Shaker*, we searched for pairs of residues between S4 and S5-P-S6 which are in frequent contact in the 100 generated models (a contact is defined as an interatomic distance less than 5 Å). The results are given in Table 2. It is observed that there are more contacts near the extracellular side than on the intracellular side. This is, in part, due to the conical (inverted teepee) shape of the pore domain. This pattern of contact suggests that experiments searching for correlated interactions between S4 and the central core might be more successful by focusing on the region near the extracellular side. Remarkably, several of the residues observed to be in contact with S4 were previously noted in the mutagenesis study of Li-Smerin et al. (2000b). In their study, they examined the residue at the "surface" of the central core S5-P-S6 constructed according to the KcsA crystallographic structure. The mutants producing large changes in gating were found to cluster near the interface between adjacent pore domain subunits. It was concluded that the voltage sensor machinery must be in contact with this region of the central pore. This is consistent with the present finding that S4 is located in this region.

The positively charged residues in S4 (R362, R365, R368, and R371) are separated by 2 residues and would not all face the same side of an α-helix. This suggests that some arginine residues must face the central core formed by S5-P-S6. Interestingly, a large number of possible contacts between S4 and aromatic side chains are observed in Table 2, such as R362 with F433, W434, and W454. It is well known that positively charged side chains (Arg, Lys, His) can associate very favorably with an aromatic side chains (Phe, Tyr, or Trp) (Gallivan and Dougherty, 1999). The interaction between isolated arginine and phenylalanine side chains (without the backbone) is about -10 kcal/mol, a value which is similar to that of simple cations with benzene in the gas phase (Sunner et al., 1981). Interestingly, mutation of F433 significantly affects gating (Li-Smerin et al., 2000b). One may also note that R362 is the only position in S4 which, upon substitution by a histidine, transforms the voltage sensor into a proton channel when *Shaker* is in its closed state (Bezanilla, personal communication). Other important aromatic residues in the interface between adjacent subunits could be F404, W434, F453, and W454. Substitution of W434 by a phenyalanine transforms the channel into a non-conducting mutant (Perozo et al., 1993). Because of the uncertainty in the 3D models, any of the residues R365, R368 and R371 could be in proximity of F404.

V. Summary

We have developed a general protocol based on a restrained molecular dynamics conformational search procedure for incorporating various kind of experimental information in the modelization of the *Shaker* K^+ channel. We have generated 100 atomic models of *Shaker* in the closed inactivated state using the currently available data. The main result of the restrained conformational search is that S4 is probably located at the interface between adjacent subunits of the central pore. This is largely consistent with the mutagenesis results of Li-Smerin et al. (2000b). Specific contacts between S4 and S5-P-S6 were found using the models generated by the conformational search which could be used to design future mutagenesis experiments. It is hoped that the present approach will help better define the 3D structure of *Shaker* as more experimental information becomes available.

References

Aggarwal, SK and R MacKinnon (1996). Contribution of the S4 segment to gating charge in the Shaker K+ channel. *Neuron*, 16:1169–1177.

Barlow, DJ and JM Thornton (1988). Helix geometry in proteins. *J Mol Biol*, 201:601–619.

Bezanilla, F (2000). The voltage sensor in voltage-dependent ion channels. *Physiol Rev*, 80:555–592.

Blaustein, RO, PA Cole, C Williams, and C Miller (2000). Tethered blockers as molecular 'tape measures' for a voltage-gated K+ channel. *Nat Struct Biol*, 7:309–311.

Bowie, JU (1997). Helix packing in membrane proteins. *J Mol Biol*, 272:780–789.

Cha, A, GE Snyder, PR Selvin, and F Bezanilla (1999). Atomic scale movement of the voltage-sensing region in a potassium channel measured via spectroscopy. *Nature*, 402:809–813.

Cortes, DM and E Perozo (1997). Structural dynamics of the streptomyces lividans K+ channel (SKC1): oligomeric stochiometry and stability. *Biochem.*, 36:10343–10352.

del Camino D, M Holmgren, Y Liu, and G Yellen (2000). Blocker protection in the pore of a voltage-gated K+ channel and its structural implications. *Nature*, 403:321–325.

Doak, DG, D Mulvey, K Kawaguchi, J Villalain, and ID Campbell (1996). Structural studies of synthetic peptides dissected from the voltage-gated sodium channel. *J Mol Biol*, 258:672–687.

Doyle, DA, JM Cabral, RA Pfuetzner, A Kuo, JM Gulbis, SL Cohen, BT Chait, and R MacKinnon (1998). The structure of the potassium channel: molecular basis of K+ conduction and selectivity. *Science*, 280:69–77.

Fiser, A, R. Sanchez, F Melo, and A. Sali (2000). Comparative protein structure modeling. In A.D. MacKerel, B. Roux, and M. Watanabe, editors, *Biological Membranes. A molecular perspective from computation and experiment*. Marcel Dekker, Inc., New York.

Gallivan, JP and DA Dougherty (1999). Cation-pi interactions in structural biology. *Proc Natl Acad Sci U S A*, 96:9459–9464.

Glauner, KS, LM Mannuzzu, CS Gandhi, and EY Isacoff (1999). Spectroscopic mapping of voltage sensor movement in the Shaker potassium channel. *Nature*, 402:813–817.

Gonzalez, C, E Rosenman, F Bezanilla, O Alvarez, and R Latorre (2000). Modulation of the Shaker K(+) channel gating kinetics by the S3-S4 linker. *J Gen Physiol*, 115:193–208.

Halsall, A and CE Dempsey (1999). Intrinsic helical propensities and stable secondary structure in a membrane-bound fragment (S4) of the shaker potassium channel. *J Mol Biol*, 293:901–915.

Haris, PI, B Ramesh, S Brazier, and D Chapman (1994). The conformational analysis of a synthetic S4 peptide corresponding to a voltage-gated potassium ion channel protein. *FEBS Lett*, 349:371–374.

Heginbotham, L, T Abramson, and R MacKinnon (1992). A functional connection between the pores of distantly related ion channels as revealed by mutant k+ channels. *Science*, 258:1152.

Heginbotham, L, Z Lu, T Abramson, and R Mackinnon (1994). Mutations in the K+ channel signature sequence. *Biophysical Journal*, 66:1061–1067.

Hille, B. (1992). *Ionic Channels of Excitable Membranes, 2nd edition*. Sinauer, Sunderland MA.

Hodgkin, A.L. and A.F. Huxley (1952). A quantitative description of membrane current and its application to conduction and excitation of nerve. *J. Physiol. (Lond.)*, 117:500–544.

Hong, KH and C Miller (2000). The lipid-protein interface of a Shaker K(+) channel. *J Gen Physiol*, 115:51–58.

Jan, LY and YN Jan (1997). Cloned potassium channels from eukaryotes and prokaryotes . *Ann Rev Neurosci*, 20:91–123.

Kobertz, WR, C Williams, and C Miller (2000). Hanging gondola structure of the T1 domain in a voltage-gated K(+) channel. *Biochemistry*, 39:10347–10352.

Li-Smerin, Y, DH Hackos, and KJ Swartz (2000a). Alpha-helical structural elements within the voltage-sensing domains of a K(+) channel. *J Gen Physiol*, 115:33–50.

Li-Smerin, Y, DH Hackos, and KJ Swartz (2000b). A localized interaction surface for voltage-sensing domains on the pore domain of a K+ channel. *Neuron*, 25:411–423.

Li-Smerin, Y and KJ Swartz (2001). Helical structure of the COOH terminus of S3 and its contribution to the gating modifier toxin receptor in voltage-gated ion channels. *J Gen Physiol*, 117:205–218.

Liman, ER, P Hess, F Weaver, and G Koren (1991). Voltage-sensing residues in the S4 region of a mammalian K+ channel. *Nature*, 353:752–756.

Liu, Y, M Holmgren, ME Jurman, and G Yellen (1997). Gated access to the pore of a voltage-dependent K+ channel. *Neuron*, 19:175–184.

Logothetis, DE, S Movahedi, C Satler, K Lindpaintner, and B Nadal-Ginard (1992). Incremental reductions of positive charge within the S4 region of a voltage-gated K+ channel result in corresponding decreases in gating charge. *Neuron*, 8:531–540.

MacKinnon, R (1991). Determination of the subunit stoichiometry of a voltage-activated potassium channel. *Nature*, 350:232–235.

MacKinnon, R, SL Cohen, A Kuo, A Lee, and BT Chait (1998). Structural conservation in prokaryotic and eukariotic potassium channels. *Science*, 280:106–109.

Monks, SA, DJ Needleman, and C Miller (1999). Helical structure and packing orientation of the S2 segment in the Shaker K+ channel. *J Gen Physiol*, 113:415–423.

Mulvey, D, GF King, RM Cooke, DG Doak, TS Harvey, and ID Campbell (1989). High resolution 1H NMR study of the solution structure of the S4 segment of the sodium channel protein. *FEBS Lett*, 257:113–117.

Papazian, DM, LC Timpe, YN Jan, and LY Jan (1991). Alteration of voltage-dependence of Shaker potassium channel by mutations in the S4 sequence. *Nature*, 349:305–310.

Perozo, E, R MacKinnon, F Bezanilla, and E Stefani (1993). Gating currents from a nonconducting mutant reveal open-closed conformations in Shaker K+ channels. *Neuron*, 11:353–358.

Richards, F.M. (1977). Areas, volumes, packing and protein structures. *Ann. Rev. Biophys. Bioeng.*, 6:151–176.

Roux, B., S. Berneche, and W. Im (2000). Ion channels, permeation and electrostatics: insight into the function of KcsA. *Biochem*, 39:13295–13306.

Sali, A and TL Blundell (1993). Comparative protein modelling by satisfaction of spatial restraints. *J Mol Biol*, 234:779–815.

Sali, A, L Potterton, F Yuan, Vlijmen H van, and M Karplus (1995). Evaluation of comparative protein modeling by MODELLER. *Proteins*, 23:318–326.

Schrempf, H, O Schmidt, R Kummerlen, S Hinnah, D Muller, M Betzler, T Steinkamp, and R Wagner (1995). A prokaryotic potassium ion channel with two predicted transmembrane segments from streptomyces lividans. *EMBO*, 14:5170.

Seoh, SA, D Sigg, DM Papazian, and F Bezanilla (1996). Voltage-sensing residues in the S2 and S4 segments of the Shaker K+ channel. *Neuron*, 16:1159–1167.

Sokolova, O, L Kolmakova-Partensky, and N Grigorieff (2001). Three-Dimensional Structure of a Voltage-Gated Potassium Channel at 2.5 nm Resolution. *Structure*, 9:215–220.

Sorensen, JB, A Cha, R Latorre, E Rosenman, and F Bezanilla (2000). Deletion of the S3-S4 linker in the Shaker potassium channel reveals two quenching groups near the outside of S4. *J Gen Physiol*, 115:209–222.

Sunner, J, K Nishizawa, and P Kebarle (1981). Ion-solvent molecule interactions in the gas phase. The potassium ion and benzene. *J Phys. Chem.*, 85:1814–1820.

Tempel, BL, DM Papazian, TL Schwarz, YN Jan, and LY Jan (1987). Sequence of a probable potassium channel component encoded at Shaker locus of Drosophila. *Science*, 237:770–775.

Tiwari-Woodruff, SK, MA Lin, CT Schulteis, and DM Papazian (2000). Voltage-dependent structural interactions in the Shaker K(+) channel. *J Gen Physiol*, 115:123–138.

Tiwari-Woodruff, SK, CT Schulteis, AF Mock, and DM Papazian (1997). Electrostatic interactions between transmembrane segments mediate folding of Shaker K+ channel subunits. *Biophys J*, 72:1489–1500.

van Schaik, RC, HJC Berendsen, AE Torda, and WF van Gunsteren (1993). A structure refinement method based on molecular dynamics in four spatial dimensions. *J. Mol. Biol.*, 234:751–762.

von Heijne G (1991). Proline kinks in transmembrane alpha-helices. *J Mol Biol*, 218:499–503.

Yellen, G (1998). The moving parts of voltage-gated ion channels. *Q Rev Biophys*, 31:239–295.

Table 1. Distance Energy Restraints

Inter-segment loops (for all subunits)		
E247 CA	F279 CA	< 25 Å
A300 CA	V311 CA	< 10 Å
A332 CA	L358 CA	< 10 Å
K380 CA	A391 CA	< 10 Å
RET measurements (all between subunit A and D, and between subunit B and C)		
V363 CB	V363 CB	within 44-46 Å
F279 CB	F279 CB	within 44-46 Å
N353 CB	N353 CB	within 36-40 Å
Salt bridge (distance taken from the nearest pair of any subunit)		
E293 OE*	K374 NZ	< 3 Å
D316 OD*	K374 NZ	< 3 Å
E283 OE*	R368 NH*	< 6 Å
E283 OE*	R371 NH*	< 6 Å
Planar restraints on ends of helices (for all subunits)		
A226 all atoms		$z < -15$ Å
E247 all atoms		$z > +15$ Å
F279 all atoms		$z > +15$ Å
A300 all atoms		$z < -15$ Å
V311 all atoms		$z < -15$ Å
A332 all atoms		$z > +15$ Å
L358 all atoms		$z > +15$ Å
K380 all atoms		$z < -15$ Å

Table 2. Residues Contacts Between S4 and S5-P-S6 from the *Shaker* Models

S4	S5 and S6						
L358	P430	D431	W434	F453	W454	K456	I457
A359	P430	F433	F453	W454	I457		
I360	P430	F433	W434	F453	W454	K456	I457
L361	F433	W434	F453	W454	I457		
R362	F433	W434	W454	I457	V458	S460	L461
V363	F433	I457	L461				
I364	I457	S460	L461				
R365	F404	I457	L461				
L366	F404	S460	L461	I464			
V367	F404	L461	I464				
R368	F404	L461	I464				
V369	F404	L461	I464				
F370	I400	F404	I464				
R371	F404						
F373	L468						
L375	L396						
R377	M393	R394	G397				
H378	M393						
S379	M393	N480					
K380	M393	E395	N480				

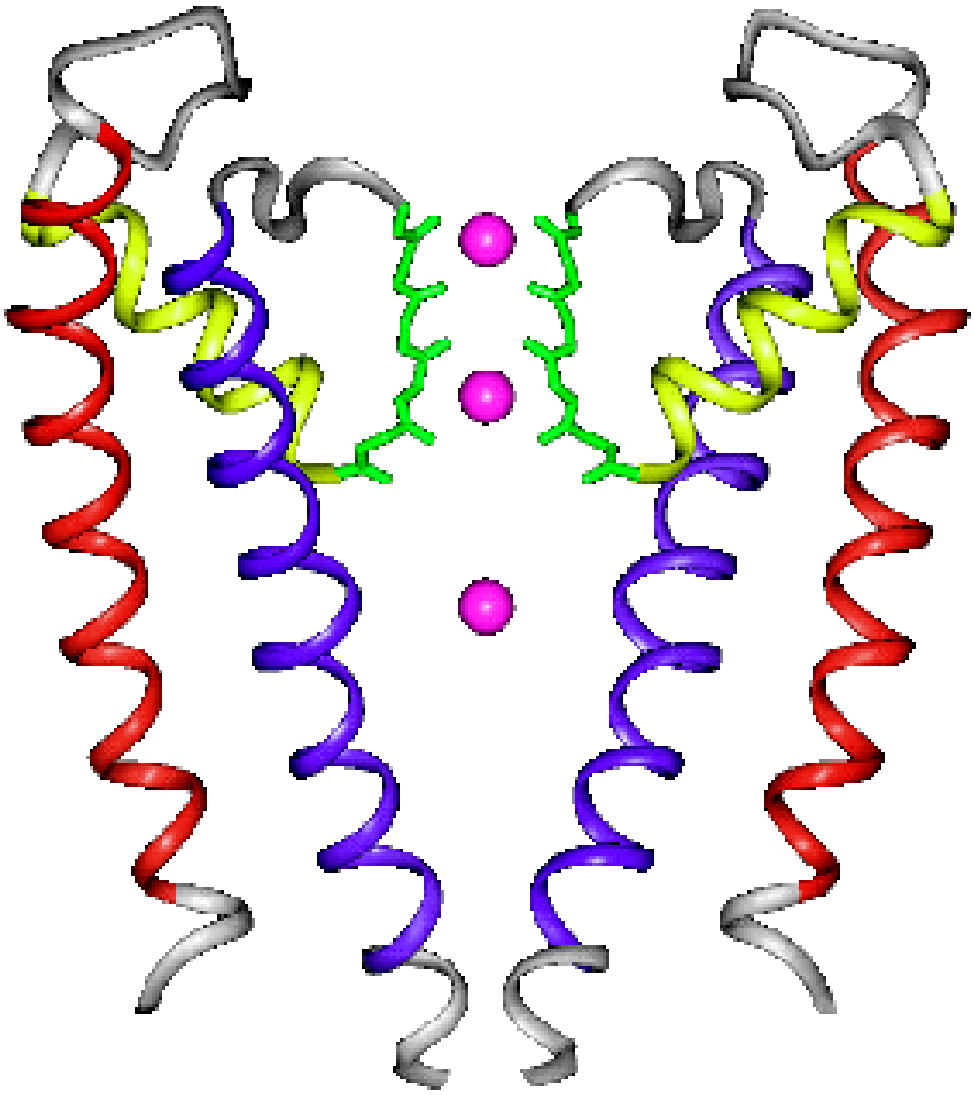

Figure 1: Schematic view of the KcsA channel (only two of the four monomers are shown). The extracellular side is at the top and the intracellular side is at the bottom. The main structural elements are: the outer helix corresponding to S5 in voltage-gated K-channels (residues by A391 to E418), the p-loop formed by the pore helix and the selectivity filter which contains the signature sequence TTVGYGD (residues I429 to T441), and the inner helix corresponding to S6 (residues G452 to N482).

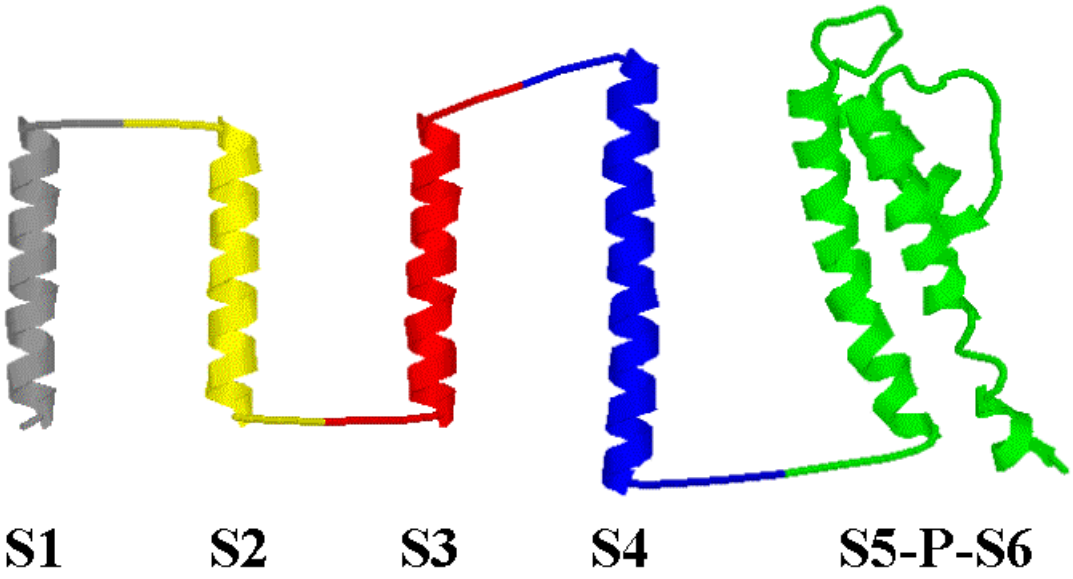

Figure 2: Schematic view of one subunit of *Shaker* with its 6 TM segments. It is assumed that S1 to S4 are in an α-helical conformation and that the central pore formed by S5-P-S6 is structurally similar to the crystallographic structure of the KcsA K^+ channel shown in Figure 1.

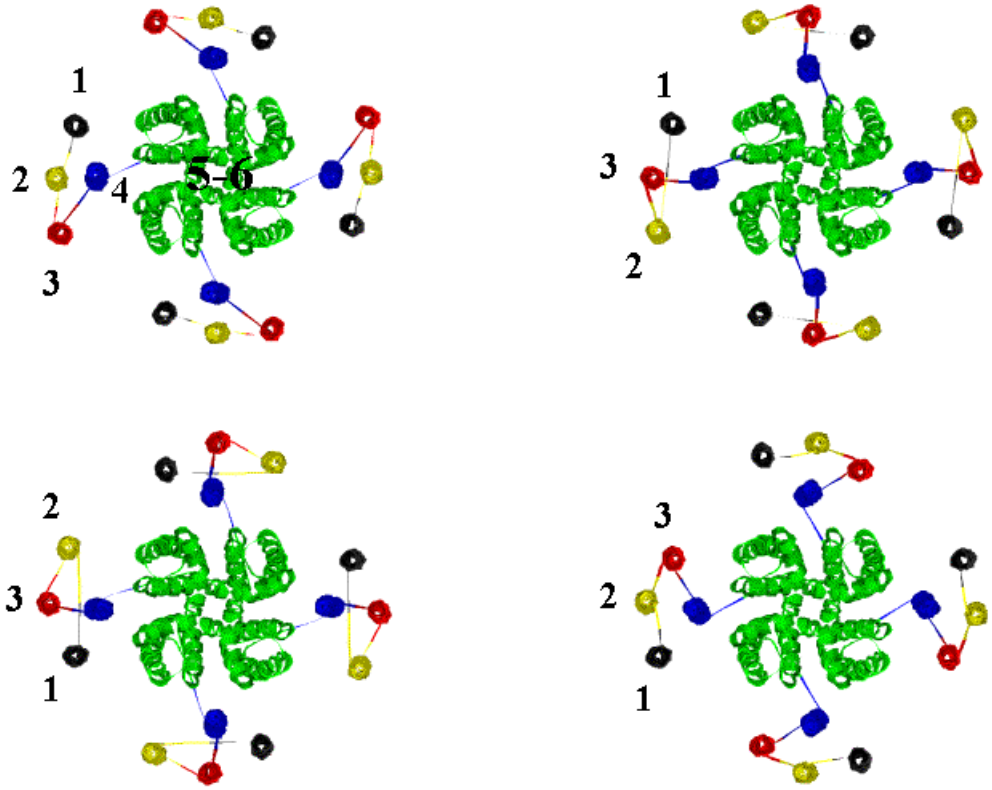

Figure 3: Example of the random initial configurations of S1 to S4 used in the conformational search.

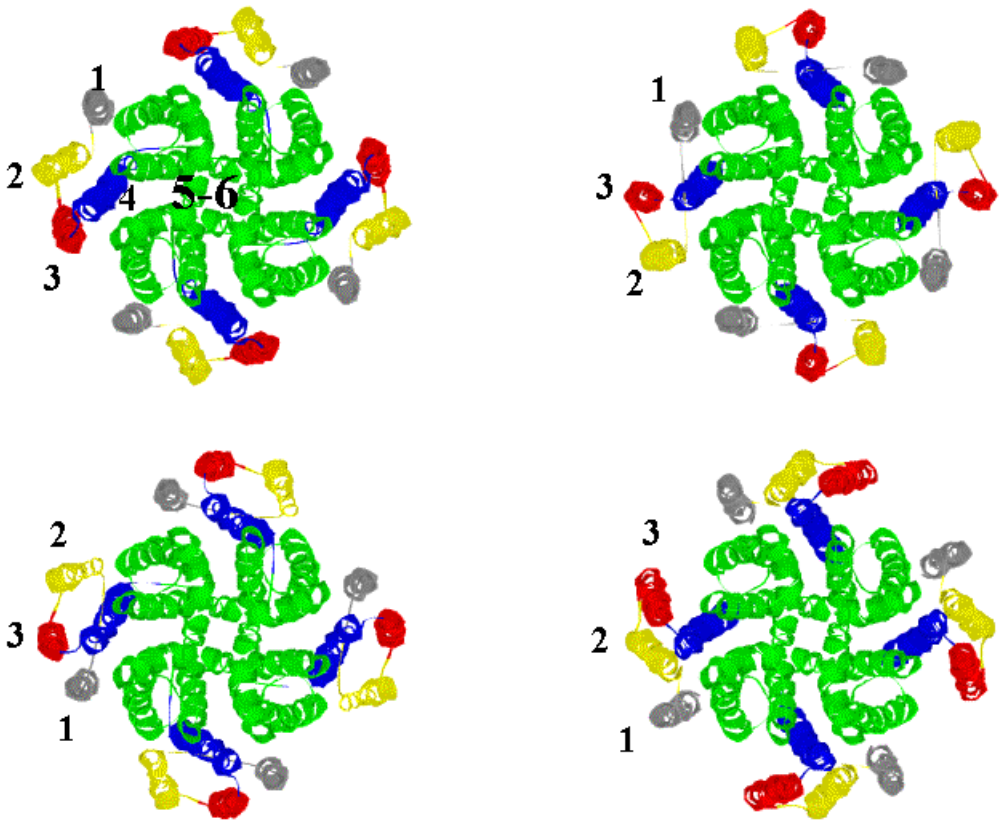

Figure 4: Example of the structural models of Figure 3 after refinement with the conformational search.

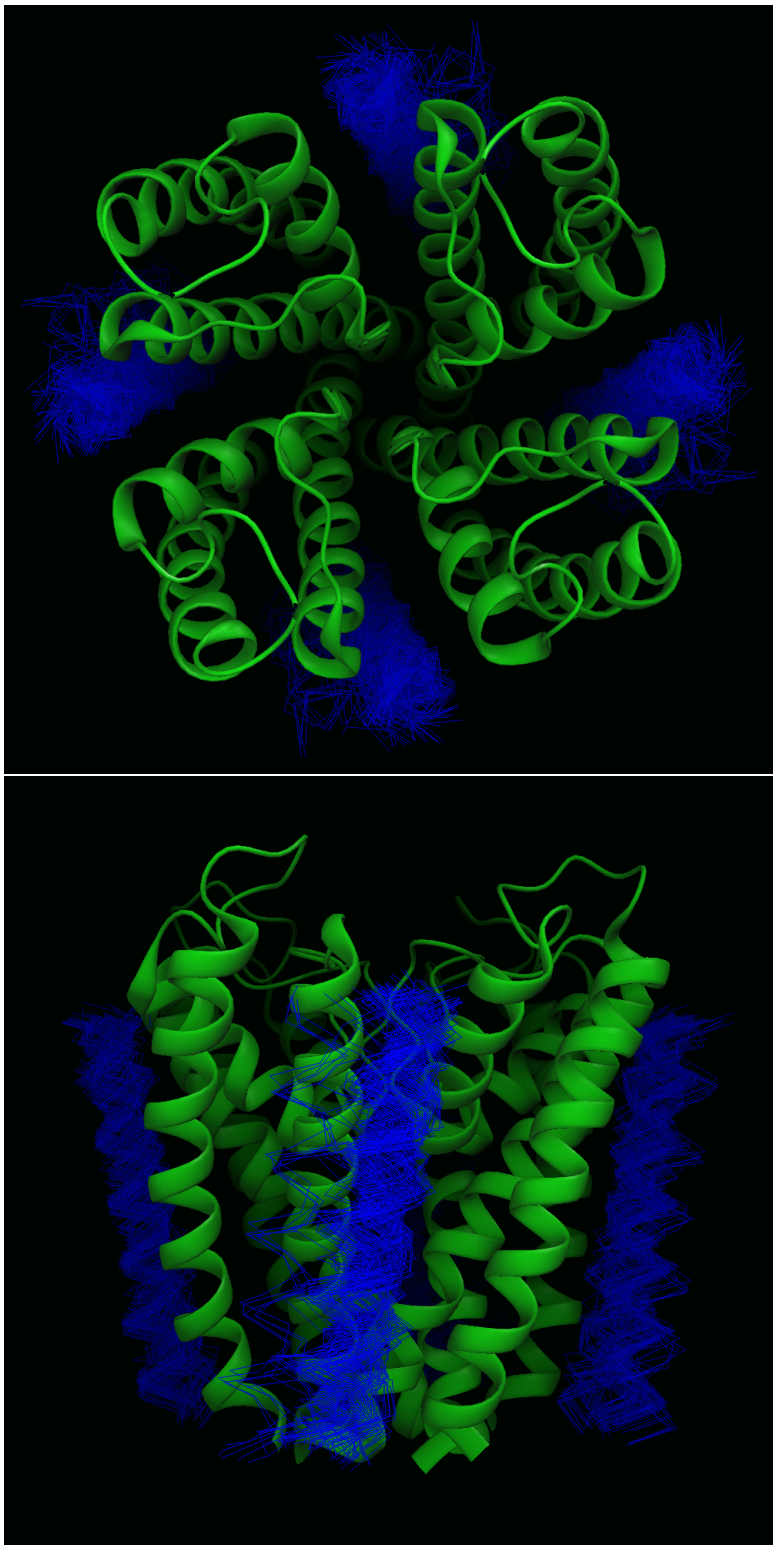

Figure 5: Superposition of the S4 segments from the 100 models with the central pore.